

## Update on $f_B$

C. Bernard,<sup>a</sup> \* T. Blum,<sup>b</sup> T. DeGrand,<sup>c</sup> C. DeTar,<sup>d</sup> Steven Gottlieb,<sup>e</sup> U. M. Heller,<sup>f</sup> J. Hetrick,<sup>g</sup>  
C. McNeile,<sup>d</sup> K. Rummukainen,<sup>e</sup> A. Soni,<sup>b</sup> R. Sugar,<sup>h</sup> D. Toussaint<sup>g</sup> and M. Wingate<sup>c</sup>

<sup>a</sup>Department of Physics, Washington University, St. Louis, MO 63130, USA

<sup>b</sup>Department of Physics, Brookhaven National Lab, Upton, NY 11973, USA

<sup>c</sup>Physics Department, University of Colorado, Boulder, CO 80309, USA

<sup>d</sup>Physics Department, University of Utah, Salt Lake City, UT 84112, USA

<sup>e</sup>Department of Physics, Indiana University, Bloomington, IN 47405, USA

<sup>f</sup>SCRI, Florida State University, Tallahassee, FL 32306-4052, USA

<sup>g</sup>Department of Physics, University of Arizona, Tucson, AZ 85721, USA

<sup>h</sup>Department of Physics, University of California, Santa Barbara, CA 93106, USA

We describe the current status of the MILC collaboration computation of  $f_B$ ,  $f_{B_s}$ ,  $f_D$ ,  $f_{D_s}$  and their ratios. Progress over the past year includes: better statistics and plateaus at  $\beta = 6.52$  (quenched),  $\beta = 5.6$  ( $N_F = 2$ ) and  $\beta = 5.445$  ( $N_F = 2$ ), new runs with a wide range of dynamical quark masses at  $\beta = 5.5$  ( $N_F = 2$ ), an estimate of the systematic errors due to the chiral extrapolation, and an improved analysis which consistently takes into account both the correlations in the data at every stage and the systematic effects due to changing fitting ranges.

Existing and planned experimental measurements of  $B$ - $\bar{B}$  and  $B_s$ - $\bar{B}_s$  mixing do not constrain the Cabibbo-Kobayashi-Maskawa matrix without knowledge of the heavy-light decay constants  $f_B$  and  $f_{B_s}$  and the corresponding  $B$ -parameters. This fact has led to a major effort in the lattice community to calculate these quantities [1].

We have been computing heavy-light decay constants with Wilson fermions over the past three years. The goal of the current stage of the computation is twofold: 1) to extrapolate the quenched results to the continuum and estimate all systematic errors within the quenched approximation, and 2) to estimate errors due to quenching by comparing, at fixed lattice spacing, results from quenched and from  $N_F = 2$  dynamical lattices.

The key ingredients in the calculation have been described in [2]. Table 1 gives the lattice parameters. Computations on the largest lattices

have been performed on the 512-node and 1024-node Intel Paragon computers at Oak Ridge National Laboratory; Paragons at Indiana University and at the San Diego Supercomputer Center have been used for smaller lattices.

We use the hopping parameter expansion of Henty and Kenway [3] for the heavy quarks. The static-light decay constants then come “for free” from the computation. However, as explained in [2], the procedure is optimized for the heavy-light case, and the static-light results are not usable when the physical volume is too large (runs B, E, and L-P). A dedicated computation of the static-light decay constants for these lattices is now in progress [4]. We use a multi-source technique, with relative wavefunctions taken from the results of the Kentucky group [5]. Since none of the weak-coupling quenched lattices (and only a subset of the coarser ones) are affected, the new running is unlikely to have much impact on the extrapolation of the quenched results to the con-

\*presented by C. Bernard

Table 1

Lattice parameters. Runs F, G, and L–P use variable-mass Wilson valence quarks and two flavors of fixed-mass staggered dynamical fermions; all other runs use quenched Wilson quarks.

| name | $\beta$ ( $am_q$ ) | size              | # configs. |
|------|--------------------|-------------------|------------|
| A    | 5.7                | $8^3 \times 48$   | 200        |
| B    | 5.7                | $16^3 \times 48$  | 100        |
| E    | 5.85               | $12^3 \times 48$  | 100        |
| C    | 6.0                | $16^3 \times 48$  | 100        |
| D    | 6.3                | $24^3 \times 80$  | 100        |
| H    | 6.52               | $32^3 \times 100$ | 60         |
| F    | 5.7 (0.01)         | $16^3 \times 32$  | 49         |
| G    | 5.6 (0.01)         | $16^3 \times 32$  | 200        |
| L    | 5.445 (0.025)      | $16^3 \times 48$  | 100        |
| N    | 5.5 (0.1)          | $24^3 \times 64$  | 100        |
| O    | 5.5 (0.05)         | $24^3 \times 64$  | 100        |
| M    | 5.5 (0.025)        | $20^3 \times 64$  | 100        |
| P    | 5.5 (0.0125)       | $20^3 \times 64$  | 100        |

tinuum. However, the  $N_F = 2$  results at stronger coupling may be significantly altered. At present, we thus base our estimate of quenching effects on a comparison with the results from run G, where the current static-light technique should be reliable and indeed gives decay constants that are consistent with the preliminary results from [4].

A major improvement in the computation over the past year is the consistent use of covariant fits at every stage of the data analysis. Previously, only the fits of  $f_{Qq}\sqrt{M_{Qq}}$  vs.  $1/M_{Qq}$  took correlations in the data into account. As is well known [6], the presence of small, poorly determined eigenvalues in the covariance matrix can make covariant fits very unstable. We therefore had been forced to use noncovariant fits to the raw correlation functions and in the chiral extrapolations.

Our new technique has many similarities to those proposed in [6], but has some advantages, at least in the current project. It is based on a standard approach in factor analysis [7]. We first compute the correlation matrix (the covariance matrix normalized with 1’s along the diagonal) and find its eigenvalues and eigenvectors. We then reconstruct the correlation matrix from

the eigenvectors, but omitting those corresponding to “small” eigenvalues. The resulting matrix is of course singular. It is made into an acceptable correlation matrix by restoring the 1’s along the diagonal. Finally, the corresponding covariance matrix is constructed and inverted, and is used in the standard way for making the fits.

The above technique interpolates smoothly between ordinary covariant fits, where no eigenvalues are omitted, and noncovariant fits, where all eigenvalues are omitted. Furthermore, because the correlation (as opposed to covariance) matrix is used, the eigenvalues are normalized, with the average eigenvalue always equal to 1. This allows us to make a uniform determination of which eigenvalues to keep, which is very important since we are dealing with thousands of fits, and it is impossible to examine each fit by hand. Our standard procedure is to keep all eigenvalues greater than 1; this accounts for typically 90–95% of the total covariance. Indeed, when one changes how the covariance matrix is computed, (for example, by changing the number of configurations eliminated in the jackknife), the eigenvalues smaller than 1 generally change drastically. The approach eliminates unstable, “pathological” fits completely. We check that the final results are not significantly affected when one keeps several more (or several fewer) eigenvalues throughout.

The use of covariant fits, with a reliable  $\chi^2$  statistic, has led to three other important changes in the analysis over the past year. First, we have found that the ranges in Euclidean time over which the smeared-local and especially the smeared-smeared correlation functions were previously fit were rather optimistic, giving  $\chi^2/dof \sim 1.5$  with 40 or 50 degrees of freedom. We now go out further in time to get reasonable confidence levels; this has increased the statistical errors somewhat and also has tended to raise the central values by about 1 (old) sigma.

A second change involves the chiral extrapolations of  $m_\pi^2$  and  $f_\pi$ . Fig. 1 shows a typical chiral extrapolation of  $f_\pi$ . The standard linear fit in  $1/\kappa$ , although apparently reasonable, has a poor confidence level once correlations in the data have been taken into account. This feature also appears in fits of  $m_\pi^2$  vs.  $1/\kappa$  and has been noted

previously in the literature [8]. Although there are no chiral logs in  $f_\pi$  in quenched chiral perturbation theory at one loop [9], nonlinear terms can enter at higher order. However, the nonlinear terms in Fig. 1 could just as easily come from  $\mathcal{O}(a)$  effects. For example, one can generally get acceptable confidence levels for linear fits to  $f_\pi$  simply by using a different quark mass definition (e.g.,  $m_1(\kappa) \equiv \ln(1 + 1/2\kappa - 1/2\kappa_c)$ ) on the horizontal axis. (Unfortunately, the curvature in  $m_\pi^2$  increases with this definition.) With just three light quark masses, we are unable to investigate such higher order effects in detail. We therefore choose linear fits in finding the central values of decay constants, and take the difference with the quadratic fits as a systematic error estimate. This is a significant ( $\sim 8\%$ ) error which we did not include previously. We note in passing that linear fits for heavy-light masses and decay constants as a function of light quark mass are generally acceptable.

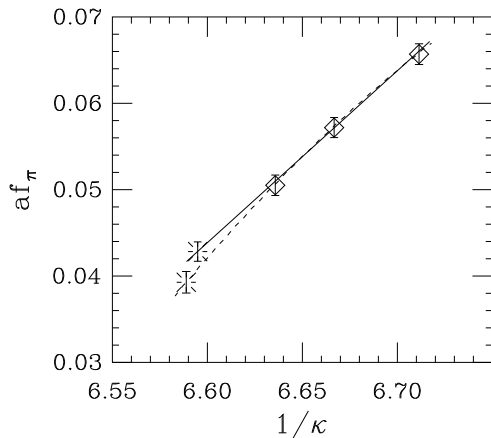


Figure 1. Fits to  $f_\pi$  vs.  $1/\kappa$  for run D. The linear fit (solid line) has confidence level 0.03; the quadratic “fit” (dashed line) has no degrees of freedom. The “bursts” show the extrapolation to  $\kappa_c$ , which in turn is determined by the corresponding fit (linear or quadratic) to  $m_\pi^2$  vs.  $1/\kappa$ .

A third change appears in the interpolation of  $f_{Qq}\sqrt{M_{Qq}}$  in inverse meson mass to  $m_B$ . A typical plot is shown in Fig. 2. When all the fits at earlier stages of the analysis are performed covariantly, the fits to the “heavier heavies” plus static

generally have higher confidence levels than fits to the “lighter heavies” plus static and are therefore used for the central values for quantities involving the  $b$  quark. On the other hand, when simple noncovariant fits are used in the earlier analysis stages, the two fits in Fig. 2 typically have comparable (and somewhat lower) confidence levels. This was the case last year, and we then chose the “lighter heavies” fit for the central values. The effect on  $f_B$  of the new choice varies with  $\beta$  in the range  $-3$  to  $+10$  MeV.

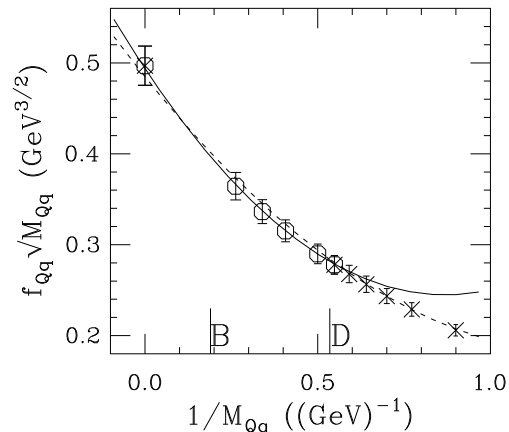


Figure 2.  $f_{Qq}(M_{Qq})^{1/2}$  vs.  $1/M_{Qq}$  for lattice D. The solid line is a quadratic fit (conf. level = 0.87) to the octagons (“heavier heavies” + static); the dashed line is a quadratic fit (conf. level = 0.37) to the crosses (“lighter heavies” + static).

The extrapolation of quenched  $f_B$  to the continuum is shown in Fig. 3. Errors on the points are larger than before [2], mainly because they now include, in addition to statistical errors, the effects of varying the fitting ranges of the raw correlators. We take the linear fit to all the quenched data (solid line) to give the central value; the dashed line gives an error estimate. An extrapolation of the  $N_F = 2$  data is not yet feasible, but may become so when we complete 1) the new static computation on the coarser lattices (L-P) and 2) new dynamical fermion runs at  $\beta = 5.6$ ,  $24^3 \times 64$ .

Figure 4 is a similar plot for  $f_{B_s}$ . Note that, although the difference at  $a \sim 0.5$  GeV between

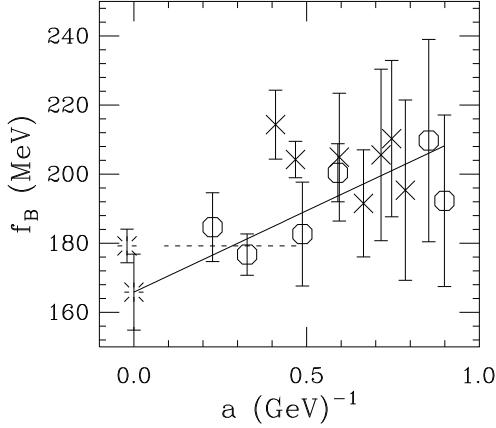


Figure 3.  $f_B$  vs.  $a$ . Octagons are quenched data; crosses,  $N_F = 2$ . The solid line is a linear fit to all quenched points (conf. level= 0.66); the dashed line is a constant fit to the three quenched points with  $a < 0.5$  GeV (conf. level= 0.76). The extrapolated values at  $a = 0$  are indicated by bursts. The scale is set by  $f_\pi = 132$  MeV throughout.

quenched and  $N_F = 2$  results for  $f_B$  is not clear, the corresponding difference seems reasonably convincing for  $f_{B_s}$ . We are hopeful that the improvements mentioned in the previous paragraph will sharpen these differences (if indeed they are present).

The analysis of systematic errors is largely unchanged from *Lattice 95* [2]. As described above, however, the errors due to chiral extrapolation are now estimated and included.

The (still preliminary) results are:

$$\begin{aligned} f_B &= 166(11)(28)(14) & f_D &= 196(9)(14)(8) \\ f_{B_s} &= 181(10)(36)(18) & f_{D_s} &= 211(7)(25)(11) \\ \frac{f_{B_s}}{f_B} &= 1.10(2)(5)(8) & \frac{f_{D_s}}{f_D} &= 1.09(2)(5)(5) \end{aligned}$$

where the first error includes statistical errors and systematic effects of changing fitting ranges; the second, other errors within the quenched approximation; the third, an estimate of the quenching error. Decay constants are in MeV. The estimate of the quenching error is crude at present and may well increase significantly when a continuum extrapolation of the dynamical fermion results is possible.

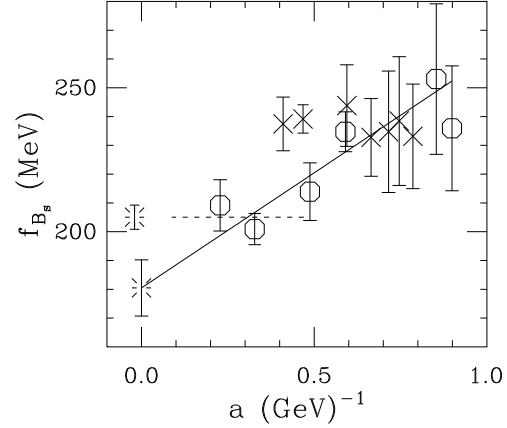


Figure 4.  $f_{B_s}$  vs.  $a$ . Points and fits as in Fig. 3. The solid line has conf. level= 0.37; the dashed line, conf. level= 0.48.

Computing was done at ORNL Center for Computational Sciences, Indiana University, and SDSC. We thank the Columbia group for supplying configurations F and the HEMCGC collaboration for configurations G. This work was supported in part by the DOE and NSF.

## REFERENCES

1. For reviews see J. Flynn, these proceedings; C. Allton, Nucl. Phys. **B** (Proc. Suppl.) **47** (1996), 31.
2. The MILC collaboration, Nucl. Phys. **B** (Proc. Suppl.) **42** (1995), 388; **47** (1996) 459.
3. D. Henty and R. Kenway, Phys. Lett. **289B** (1992) 109.
4. The MILC collaboration (presented by C. McNeile), these proceedings.
5. T. Draper and C. McNeile, Nucl. Phys. **B** (Proc. Suppl.) **34** (1994), 453.
6. B. Thacker and G.P. Lepage Phys. Rev. **D43**: (1991) 196; G. Kilcup, Nucl. Phys. **B** (Proc. Suppl.) **34** (1994), 350; C. Michael, Phys. Rev. **D49** (1994) 2616.
7. H. H. Harmon, *Modern Factor Analysis*, 2nd ed., Univ. of Chicago Press, 1967, chapter 8.
8. T. Bhattacharya and R. Gupta, Phys. Rev. **D54** (1996) 1155.
9. C. Bernard and M. Golterman, Phys. Rev. **D46** (1992) 853 and references therein.